

Model Description

This model covers the full spherical shell of the solar interior ($0 \leq \theta \leq \pi$, $0 \leq \phi \leq 2\pi$, $0.61R \leq r \leq 0.96R$). We solve the following anelastic incompressible MHD equations for varying resolutions, with the following sets of grid points: (512 ϕ , 256 θ , 256 r), (256 ϕ , 128 θ , 128 r) and (128 ϕ , 64 θ , 64 r).

$$\nabla \cdot (\rho_s u) = 0$$

$$\frac{Du}{Dt} + 2\Omega \times u = -\nabla \left(\frac{p'}{\rho_s} \right) + g \left(\frac{\Theta'}{\Theta_s} \right) + \frac{1}{\mu_0 \rho_s} (B \cdot \nabla) B$$

$$\frac{D\Theta'}{Dt} = -u \cdot \nabla \Theta_c - \frac{\Theta'}{\tau}$$

$$\frac{DB}{Dt} = (B \cdot \nabla) u - B(\nabla \cdot u)$$

In these equations, D/Dt is the total time derivative (or material derivative), u is the velocity field in the rotating frame Ω , p' is the fluctuating pressure term for both the gas and magnetic pressure, Θ' represents the potential temperature fluctuations from an ambient state (Θ_c), ρ_s and Θ_s are the density and potential temperature of the isentropic reference state. The term Θ'/τ maintains a steady, axisymmetric solution of the stellar structure against the action of convective turbulent motions induced by the ambient state Θ_c .

The ambient state is a polytropic ideal gas model with a polytropic index of $\gamma = 1.499978$ in the convective zone and $\gamma = 2$ in the radiative zone. For the low resolution models we change the index at the very surface to be $\gamma = 1.5$ (ns1), $\gamma = 1.8$ (ns2), and $\gamma = 1.499975$ (ns3). These equations are all solved numerically with the EULAG-MHD code following an MPDATA formulation (Ghizaru et al. 2010; Racine et al. 2011; Smolarkiewicz & Charbonneau 2013; Guerrero et al. 2013), which is a spin-off of the hydrodynamical model EULAG predominantly used in atmospheric and climate research (Prusa et al. 2008). For the velocity field we use impermeable, stress-free boundary conditions. For the magnetic field we only allow the existence of a radial field on the boundaries.

Visualizations

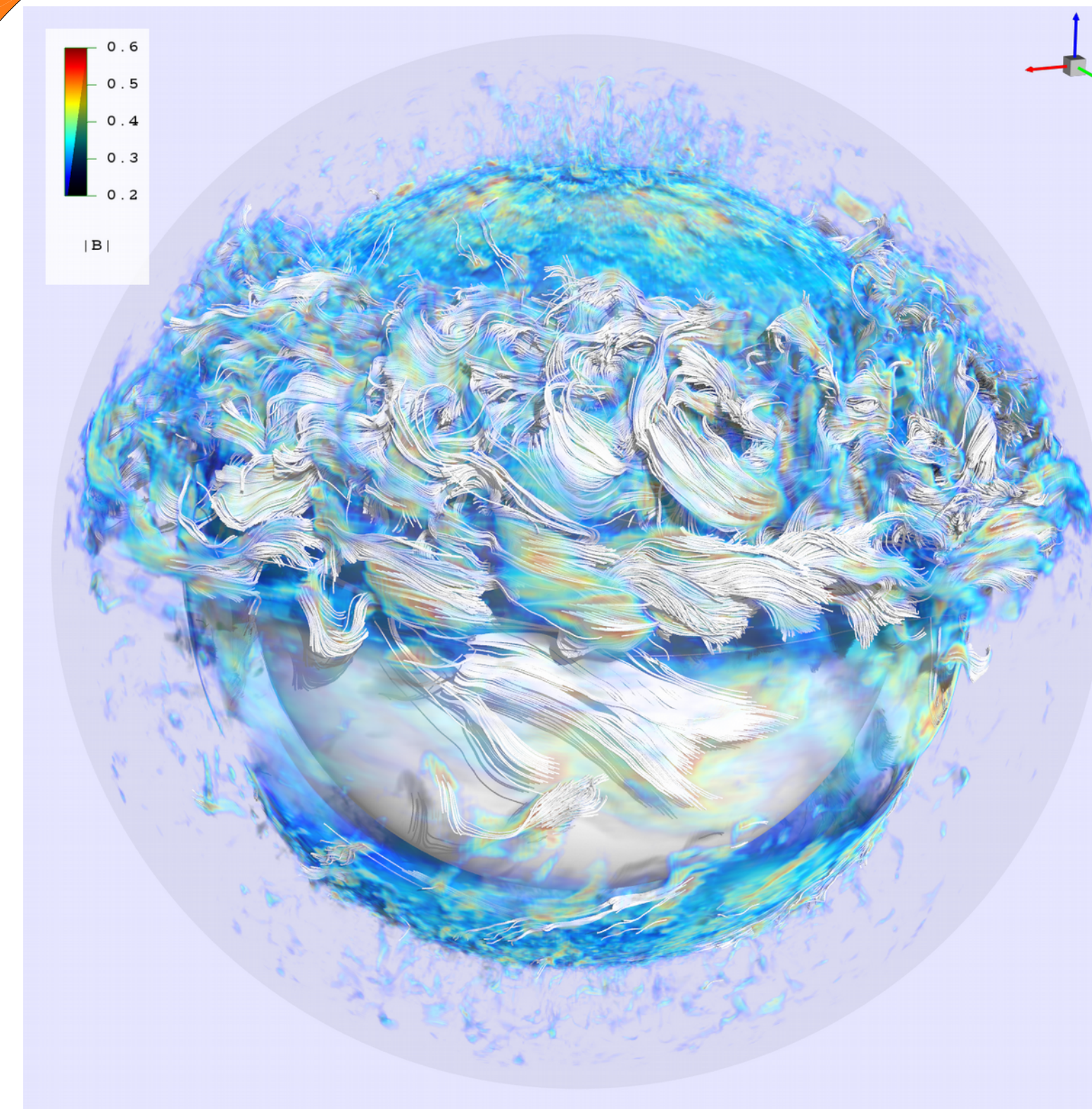


Figure 4. Above, we can see a snapshot of the magnitude of the magnetic field in color with magnetic field lines drawn in white on a high resolution model (512 ϕ , 256 θ , 256 r).

Image credit: Timothy Sandstrom

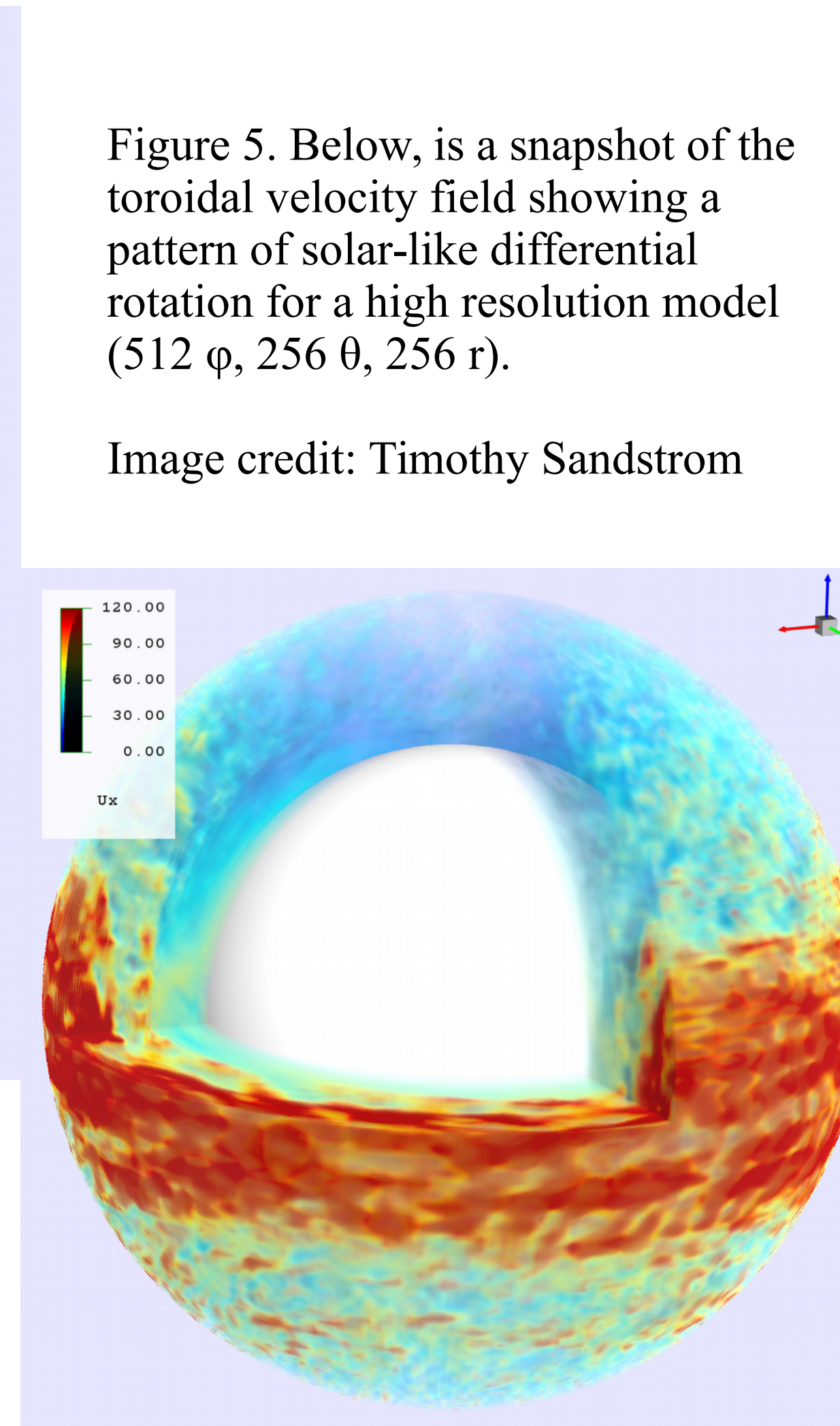


Figure 5. Below, is a snapshot of the toroidal velocity field showing a pattern of solar-like differential rotation for a high resolution model (512 ϕ , 256 θ , 256 r).

Image credit: Timothy Sandstrom

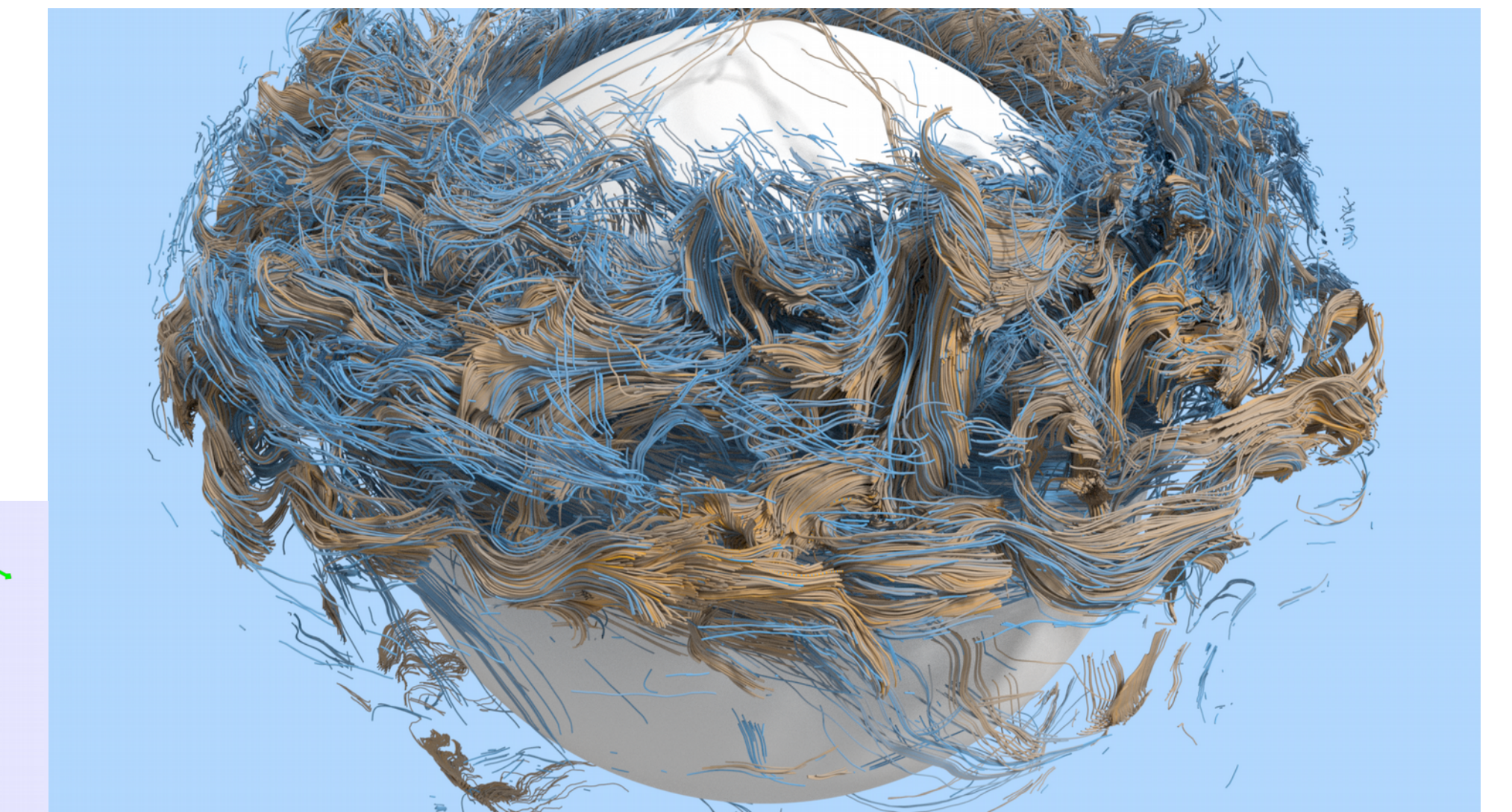


Figure 6. Above, is a snapshot of the same magnetic field as shown in Fig. (4), with the total magnitude of the field removed and magnetic field lines colored based on polarity for the high resolution model (512 ϕ , 256 θ , 256 r).

Image credit: Timothy Sandstrom

Near-Surface Models

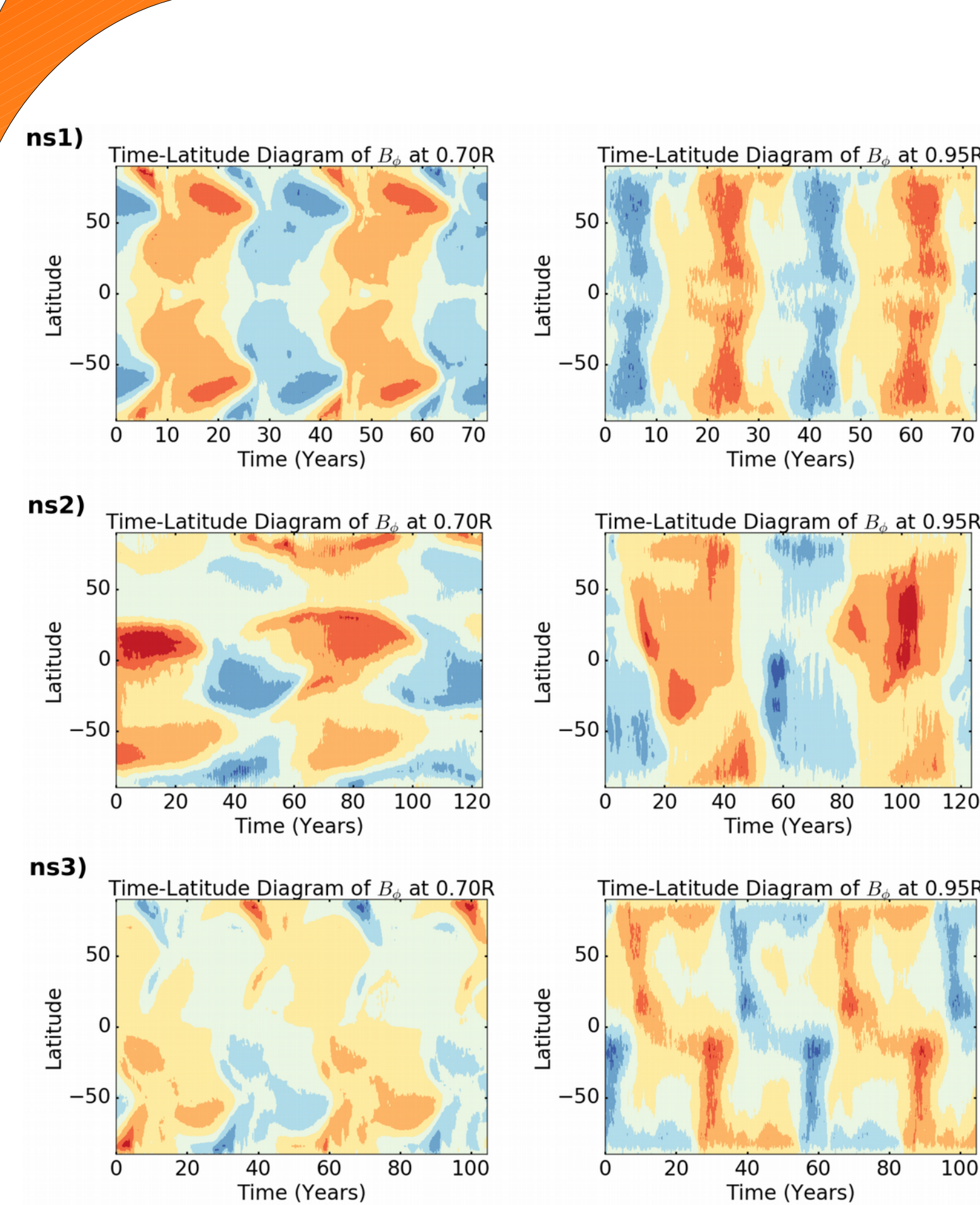


Figure 2. The time-latitude diagrams for the toroidal magnetic field (B_ϕ) of ns1, ns2, and ns3 (128 ϕ , 64 θ , 64 r) at $0.70 R_\odot$ on the left and $0.95 R_\odot$ on the right.

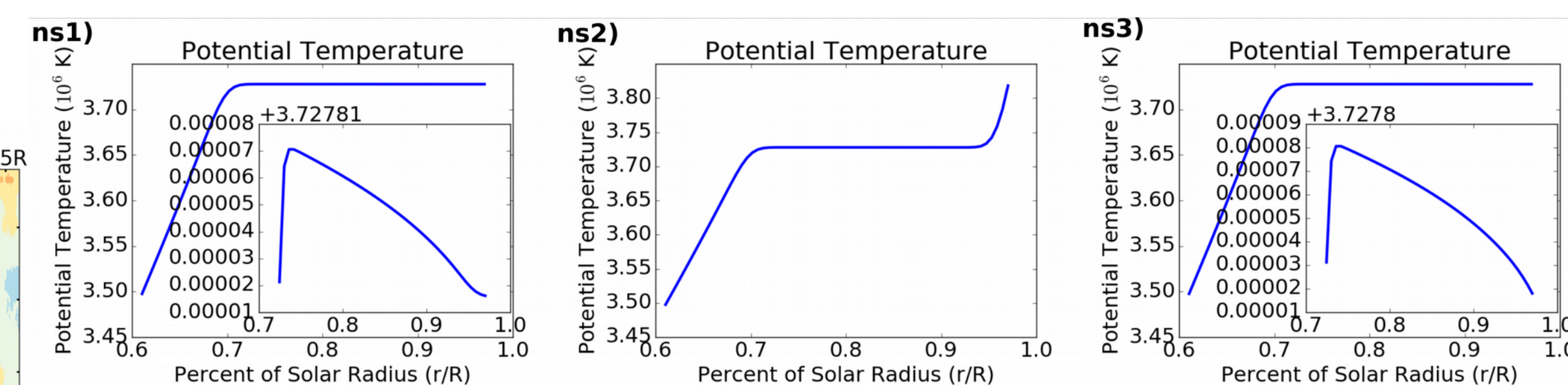


Figure 1. The potential temperature (Θ) profiles for ns1, ns2, and ns3.

For the low resolution models (128 ϕ , 64 θ , 64 r), when a tachocline was incorporated the duration and pattern of the magnetic cycle began to match the 11-year cycle we see on the Sun more closely (Guerrero et al. 2013, 2015). These results showed us that regions of large velocity shear such as the tachocline and the near-surface shear layer can have dramatic effect on the global cycle. To test this we decided to implement various levels of convection at the surface to induce different regimes of shear (Fig. 1), where ns1 is slightly altered to reduce convection at the surface, ns2 has very strongly suppressed convection and ns3 has increased convection in a more typical solar-like fashion. In Fig. (3) we see the effect on the velocity field. The meridional profiles seem to be consistently conserved in a 2 cell structure, but in the differential rotation profiles, as we approach solar-like convection parameters, the radiation zone speeds up close to the rate of rotation at the equator which is similar to what we observe on the Sun. This may be a consequence of parcels of plasma hitting the tachocline with greater speeds. We also see very interesting differences in patterns exhibited by the magnetic fields. In Fig. (2) we can see that when we suppress convection it will result in the completely symmetric cycle shown in ns1 and ns2, however, when we increase surface convection, the structure of the field changes drastically into the type of non-axisymmetric pattern that we see on the Sun.

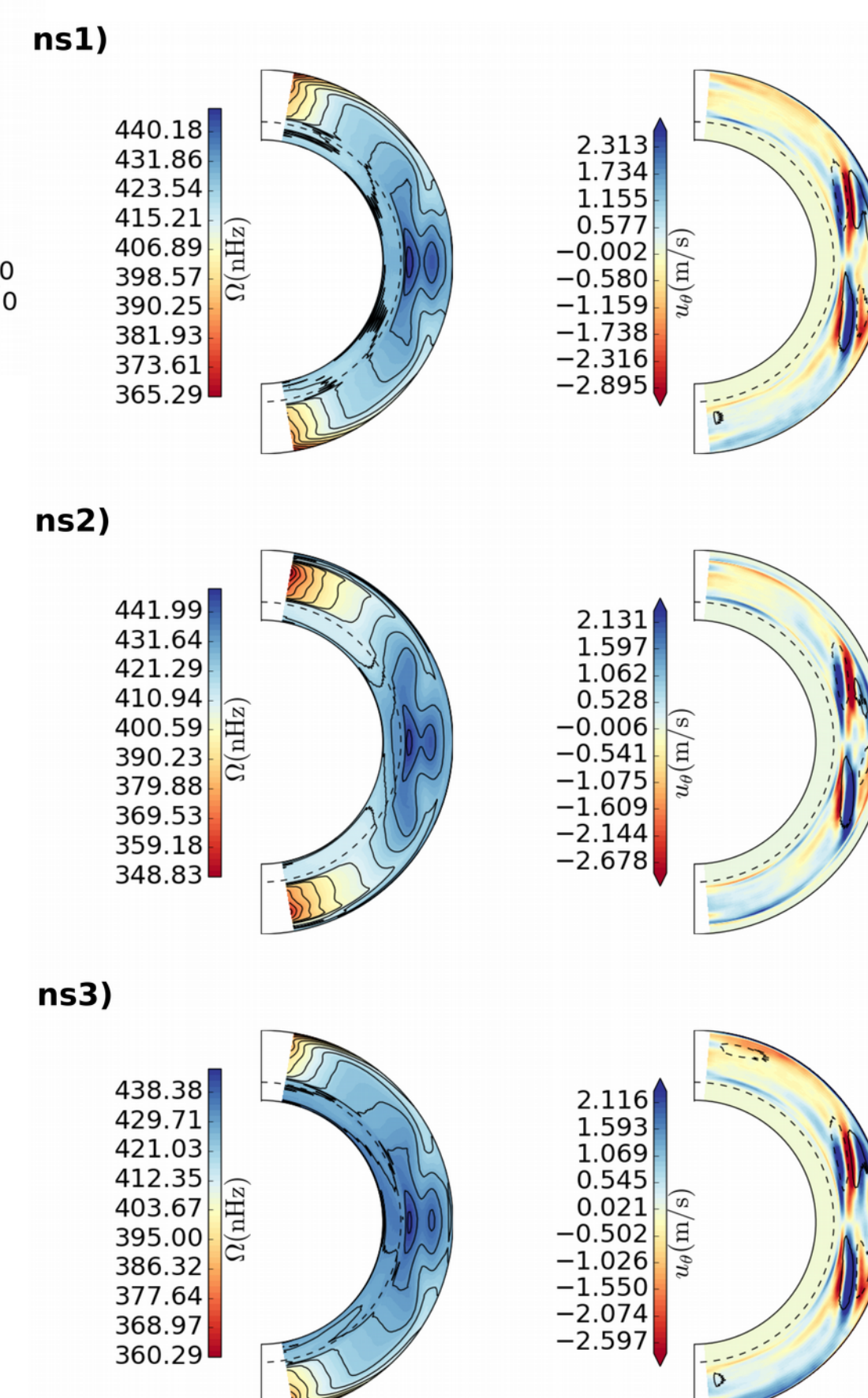


Figure 3. The differential rotation and meridional circulation profiles for ns1, ns2, and ns3 (128 ϕ , 64 θ , 64 r).

Conclusions

Increasing the resolution of the models gave us some interesting, but not completely trustworthy results. This model uses an implicit viscosity formulation (ILES) where the numerical viscosity depends on the truncation error, which means that we can get drastically different results at different resolutions. We have found that at lower resolutions (128 ϕ , 64 θ , 64 r), the ILES scheme produces turbulent dissipation that gives us results that are similar to what we observe on the Sun, while for higher resolutions the error in implicit viscosity is too great, and any meaningful results that we can interpret will be significantly diluted by error. Another large issue is that running high resolution models puts a strain on resources, as they take a very long time to compute - 5 to 10 times longer than the lower resolution models. The high resolution models do however give us an incredible opportunity to observe the formation and evolution of magnetic structures directly, which may not give us much confidence in a particular result, but can give us a better understanding of the patterns of flow and the nature of magnetic structures.

The low resolution models, however, gave us some very interesting results. These models exhibit a much more accurate representation of plasma flow on the sun with a viscosity that creates a much more solar-like distribution in differential rotation and meridional circulation, which can help generate semi-accurate accurate solar cycles (Guerrero et al. 2013, 2015). With the inclusion of the tachocline and parts of the near-surface shear layer, the magnetic field can achieve a solar cycle nearing the decade long period we observe on the Sun. There are, however, still significant problems as we do not model the near-surface shear very realistically and are missing the top 4% of the Sun. In our work we saw that small differences in this upper layer can create huge changes in the global dynamo, so in our future work we are planning a model that can be extended to the surface and that can accurately simulate the turbulence, compression and shear in this upper layer.

Bibliography

- Ghizaru, M., Charbonneau, P., & Smolarkiewicz, P. K. 2010, ApJL, 715, L133
 Guerrero, G., Smolarkiewicz, P. K., Kosovichev, A. G., & Mansour, N. N. 2013, ApJ, 779, 176
 Guerrero, G., Smolarkiewicz, P. K., de Gouveia Dal Pino, E. M., Kosovichev, A. G., & Mansour, N. N. 2015
 Prusa, J. M., Smolarkiewicz, P. K., & Wyszogrodzki, A. A. 2008, Comput. Fluids, 37, 1193
 Racine, E., Charbonneau, P., Ghizaru, M., Bouchat, A., & Smolarkiewicz, P. K. 2011, ApJ, 735, 46
 Smolarkiewicz, P. K., & Charbonneau, P. 2013, J. Comput. Phys., 236, 608